Letters in Applied NanoBioScience
Open-Access Journal (ISSN: 2284-6808)

Article
Volume 15, Issue 2, 2026, 73
https://doi.org/10.33263/LIANBS152.073

Enhanced Antibacterial Activity of TiO_2 Nanoparticles Synthesized Using HCl-Assisted Methods

Muna Alhilly [1], **Ammar S. Hameed** [1,*]

[1] Department of Physics, College of Science, University of Kerbala, Karbala, Iraq
* Correspondence: ammar.s@uokerbala.edu.iq;

Received: 4.04.2025; Accepted: 22.02.2026; Published: 30.06.2026

Abstract: Titanium dioxide (TiO_2) is widely recognized for its photocatalytic antibacterial activity, offering a sustainable solution for microbial control in diverse applications. TiO_2 nanoparticles prepared using the solvothermal method. Titanium butoxide as a raw material in a dilute hydrochloric acid solution at different concentrations. The parameters, such as reaction time and hydrochloric acid amount, were used to control the size of nanoparticles and quantity. TiO_2 NPs were characterized using X-ray diffraction, field emission scanning electron microscopy (FESEM), energy dispersive X-ray spectroscopy (EDX), and Zeta potential analysis. X-ray proved a tetragonal structure in a rutile phase, and the average crystal size decreased (41 to 20) nm when increasing the amount of HCl from 1 ml to 1.5 ml. Also, the grain size decreased (41 to 28) nm when the amount of HCl increased, as shown in FESEM results. TiO_2 nanoparticles sample (H2) showed a strong antibacterial effect against both gram-negative bacterium *Escherichia coli* (51 ± 0.2 mm) and gram-positive bacterium *S. aureus* (26 ± 0.4 mm), which proved excellent results.

Keywords: TiO_2 NPs; antibacterial activity; HCl.

1. Introduction

Titanium dioxide (TiO_2) has garnered significant attention as a potent antibacterial agent due to its unique photocatalytic properties [1]. Under ultraviolet (UV) light, TiO_2 generates reactive oxygen species (ROS) [2], such as hydroxyl radicals and superoxide anions [3,4], which exhibit strong oxidative activity capable of destroying bacterial cell walls and inhibiting microbial growth [5,6]. There is significant scientific interest in techniques that reduce or eliminate bacterial growth [7]. As bacteria have become increasingly resistant to some antibiotics, their toxicity and harm to the human body have increased [8]. The aspiration has begun towards nanotechnology through metals, their oxides [9], and compounds which have been distinguished by a dramatic change in their optical [10], electrical, electronic, and mechanical properties [11]. Moreover, the nanotechnology has further enhanced the antibacterial efficacy of TiO_2 by increasing its surface area [12,13] and tailoring its properties to extend its activity under visible light. This can be achieved by reducing particle size to the nanoscale, which in turn leads to a significant increase in the surface area-to-volume ratio [14], a ratio on which the antibacterial effect depends [15]. The most prominent properties of titanium oxides (TiO_2) are being a transitional semiconductor [16], which has invaded the medical, industrial, and commercial sectors due to its advantages, such as being a strong

photocatalyst [17], chemically stable [18], relatively cheap, and environmentally friendly [19]. Moreover, it has been widely used as an antibacterial due to its good oxidation and reduction properties [20]. Additionally, the inertness and high biocompatibility of titanium dioxide nanoparticles with human tissues make them an interesting material for bacterial activity compared to other metals and oxides [21]. Despite the advantages of TiO_2, it has some drawbacks, such as its wide bandgap (Eg≈3 eV). The exposure of TiO_2 nanoparticles to ultraviolet (UV) radiation provided the energy required to cause the electron to transfer from the valence band to the conduction band. This condition lead to create an electron-hole pairs [22] which lead to low visible light absorption and the fast charge recombination rates [23] that considerably decrease the quantum yields of the photoreactions.

Furthermore, titanium dioxide exists in three crystalline forms: anatase, rutile, and brookite [24], with band gap energies of 3.2, 3.0, and 2.96 eV, respectively [24]. The crystal structure and morphology of titanium dioxide nanoparticles are affected by temperature and acidity concentration, which, in turn, affect the physical and chemical properties associated with the antibacterial effect [25]. Therefore, the physical, chemical, and antibacterial properties of the titanium dioxide nanoparticles are influenced by the synthesis method. To obtain highly crystalline titanium dioxide nanoparticles with small crystal size [9], a high specific surface area, defect-free properties, and low agglomeration are required [26]. Therefore, solvothermal method has been used for synthesis of TiO_2 which involves experimental parameters such as temperature, solvent type [14], pH of titanium precursor [25], and reaction time to control the properties of titanium dioxide nanoparticles. Where the use of HCl in the synthesis process was employed to tune the physicochemical properties of TiO_2 nanoparticles. Its role in controlling hydrolysis and influencing crystal structure was found to be significant [27,28]. This approach was considered novel compared to traditional synthesis methods. Moreover, this method requires elevated temperature and pressure, which improve the solubility of the starting material [29]. Furthermore, the main process of Titanium Oxidation is the nucleation which consists of several stages, starting with the process of decomposition of the raw material, which is Titanium Butoxide $Ti(OBu)_4$, by reacting with water H_2O as a solvent and HCL as catalyst to produce titanium hydroxide ($Ti(OH)_4$), which in turn combines with its counterpart by the process of dehydration after obtaining Hydrogen ion (H+) from HCL. Finally, $Ti(OBu)_4$ reacts with water H_2O to form TiO_2 nucleus with butanol alcohol (4BuOH) as end product [30].

as per chemical reaction (HCl(catalyst)), (R= Bu=C_4H_9):

$$\text{Hydrolysis: } Ti(OR)_4 + 4H_2O \xrightarrow{HCl} Ti(OH)_4 + 4ROH \quad (1)$$

$$\text{Dehydration: } Ti(OH)_4 + Ti(OH)_4 \rightarrow 2TiO_2 + 4H_2O \quad (2)$$

$$Ti(OH)_4 + Ti(OR)_4 \rightarrow 2TiO_2 + 4ROH \quad (3)$$

The entire reaction via the hydrothermal process between the TBO precursor and water is controlled, including structure and growth [31].

$$Ti(OR)_4 + 2H_2O \rightarrow TiO_2 + 4ROH \quad (4)$$

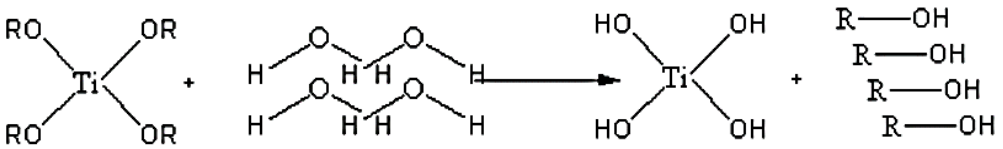

(a)

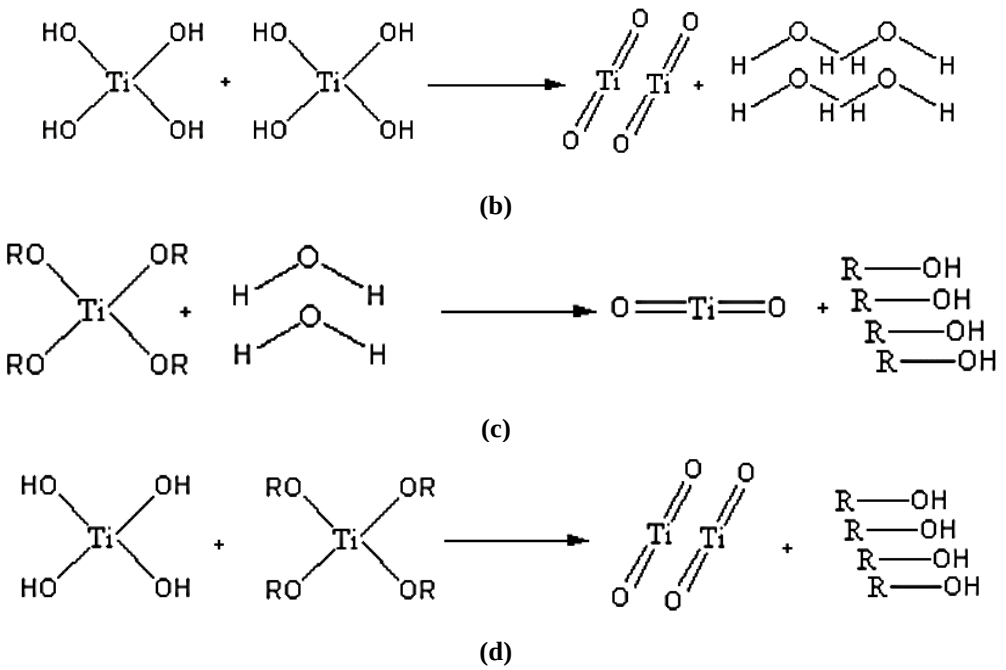

Figure 1. Reaction mechanism of rutile growth during: **(a)** Hydrolysis process; **(b)** Dehydration process; **(c)** Union and **(d)** formation process of the molecules[30].

In terms of antimicrobial activity, Titanium dioxide nanoparticles stimulated by photo-induced reaction with ultraviolet light (< 385nm), leading to a chemical imbalance in the cell wall of the bacteria. The electrons generated by the excited particles react with cellular components such as water (H_2O), oxygen (O_2), and hydrogen (H), leading to the production of reactive oxygen species (ROS), including hydrogen peroxide (H_2O_2), superoxide anion ($\cdot O_2^-$), and hydroxyl radical (OH). These ROS are produced at levels higher than normal and can damage all parts of the (Gram-negative bacteria and Gram-positive bacteria) cell, including DNA, mitochondria, cytoplasm, and proteins, as well as the cellular machinery responsible for protein synthesis, ultimately leading to cell destruction, as illustrated in Figure 2 [32-34]. Therefore, the mechanism of antibacterial activity of nano-titania depends on its photocatalytic reaction. The mechanism of radicals' generation (OH and $O2^-$) is presented as follows [14,35]:

$$TiO_2 + h\nu \rightarrow TiO_2\,(e^- + h^+) \quad (5)$$

$$H_2O + TiO_2\,(h^+) \rightarrow TiO_2 + \cdot OH + H^+ \quad (6)$$

$$O_2 + TiO_2\,(e^-) \rightarrow TiO_2 + \cdot O_2^- \quad (7)$$

$$H_2O + \cdot O_2^- \rightarrow OOH\cdot + OH \quad (8)$$

$$2OOH\cdot \rightarrow O_2 + H_2O_2 \quad (9)$$

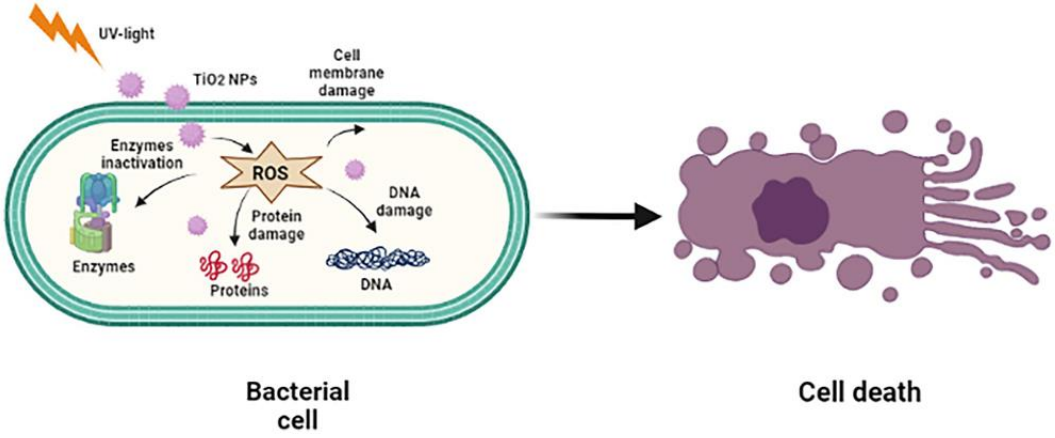

Figure 2. Antibacterial action mechanism of TiO_2 nanoparticles [36].

This study aimed to investigate the effect of hydrochloric acid (HCl) on the synthesis of TiO_2 nanoparticles and to evaluate its role in tuning their structural and morphological properties for enhanced functional performance. Also, to investigate the antibacterial efficacy of TiO_2 nanoparticles under visible light conditions against common bacterial strains, including *Escherichia coli* and *Staphylococcus aureus*.

2. Materials and Methods

All the materials used in the present research were obtained from Sigma -Aldrich Chemicals which are: Titanium (IV) butoxide [TBOT] (with M.Wt = 284.2 g mol^{-1},purity=97%) as aTiO_2 precursor, Distilled water(DW), Hydrochloric Acid [HCl] from J.T.Baker Chemicals (36.5 -38 %), and Absolute Ethanol [C_2H_5OH] from J.T. Baker Chemicals (M.Wt=46.07 g mol^{-1}, purity=99.9%).

Titanium dioxide nanoparticles (TiO_2-NPs) were prepared by using a solvothermal process in which titanium butoxide ($Ti(OBu)_4$) was used as a precursor [37] (starting material), hydrochloric acid (HCl) as a chelating agent, and Deionized water (DW) as a solvent. Hydrochloride solvent was prepared by diluting the hydrochloric acid (in ratios 0.75, 1, 1.5) ml HCl: 39ml DW) with distilled water by mixing for 5 minutes (by a magnetic stirrer device with speed 400 rpm) as step one. Then 1 ml titanium butoxide ($Ti(OBu)_4$) was added dropwise (to avoid clumping) into the hydrochloric solvent. After 15 min of mixing (with a speed of 400 rpm), the formation of a transparent liquid is shown in Figure 1. After one night in laboratory conditions (avoid the light), step three is started by heating and mixing the sample [to 75°C, 400 rpm], and after (1.5,1,0.5) hours, the change in the color from clear to white, which is considered evidence of the emergence of TiO_2 nanoparticles. From here, TiO_2 nanoparticles are separated from the solution by centrifuging (for 10 min and 4000 rpm) to produce the required material. After that, all samples have been adjusted by (DW) to get the appropriate PH, and this process is repeated more than once until the PH reaches neutrality (when PH=7). Then, the sample is dried at 95°C using a heater. After that, the sample is calcified in the electrical furnace maintained at 450°C for 2 h. Finally, the electrical furnace is left to cool naturally to room temperature. The experimental details are listed in Table 1.

Table 1. The preparation conditions of TiO_2 nanorods.

Sample	Structer	HCl to distilled water ratio	
H	TiO_2	39 DW:0.75 ml HCL	Ti(OBu)4 volume for all Sample 1 ml
H1	TiO_2	39 DW:1 ml HCL	
H2	TiO_2	39 DW:1.5 ml HCL	

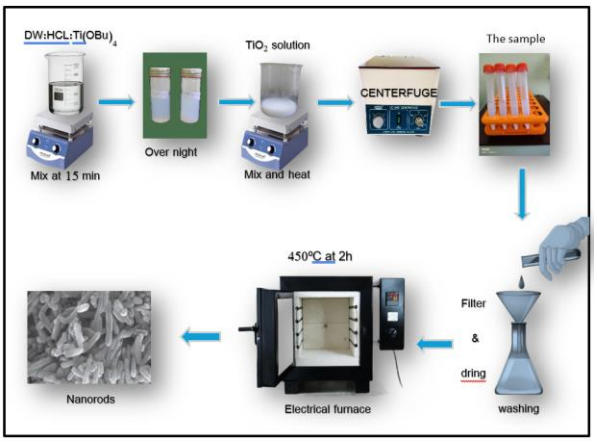

Figure 3. Schematic diagram of the steps of the synthesis of TiO_2 by the solvothermal method.

2.1. Characterization of TiO_2 nanoparticles.

Using several techniques, titanium dioxide nanoparticles can be characterized, such as the XRD technique, which provided the structural phases and crystal size of (TiO_2-NPs). The FESEM technique can be used to examine the surface morphology of nanoparticles and the particle distribution of TiO_2 NRs, in addition to the EDX technique, which is used to determine the chemical composition. Finally, the technique of Zeta potential is an important technique for calculating the surface charge of nanoparticles (TiO_2 -NPs).

2.2. Antibacterial activity test.

The antibacterial potential of the prepared samples (H, H1, H2) was investigated against Gram-negative and Gram-positive bacterial strains using the agar well diffusion assay. About 20 mL of Muller–Hinton (MH) agar was aseptically poured into sterile Petri dishes. The bacterial species were collected from their stock cultures using a sterile wire loop [38]. After culturing the organisms, 6 mm-diameter wells were bored on the agar plates using a sterile tip. Into the bored wells, different concentrations of the samples (H, H1, H2) were used. The cultured plates containing the samples (H, H1, H2) and the test organisms were incubated overnight at 37°C before measuring and recording the average zone of inhibition diameter. where the test was performed in five replicates for each sample, and the average diameter of the inhibition zones was measured using Agar Diffusion assays and ImageJ/Fiji, a free and open-source image analysis program.

3. Results and Discussion

3.1. Structural properties of TiO_2 NRs.

Valuable information on structures, phases, preferred crystalline orientations, and average crystallite/grain size of TiO_2 nanoparticles can be provided using XRD technical [39]. The examination of the samples usually takes place for 2θ values between 10.02º and 79.98º with a step size of 0.046º and time exposed to radiation of about 1 sec per step. The rutile phase of TiO_2 was a tetragonal crystalline system. Figure 4 shows characteristic diffraction peaks of H1 such as (110), (210), (111), (211), (220), (301) and (202) at 2θº=27.37º, 43.97º, 41.23º, 54.32º, 56.44º, 68.96º and 76.25º those that match the standard values of (JCPDS card number 01-077.0441) In addition to a slight deviation in some peaks (200), (002), (212) Finally, the most intense peak is (110) at 2θº=27.37º. Peaks H2 sample are (110), (101), (200), (111), (210), (211) and (220) at 2θº=27.38º, 36.28º, 39.17º, 41.55º, 44.38º, 54.61º and 56.83º those that match the standard values of (JCPDS card number 01-088-1172). From observing Tables 2,3, a correlation between the maximum peak width, intensity, and crystal size was determined by:

$$D \propto \text{peak intensity}/\text{FWHM} \qquad (10)$$

Therefore, the FWHM had smaller values in Table 2 than the values of FWHM in Table 3. That is, the wider peaks mean that the crystal size is smaller, and the relationship is direct between the acid concentration and the FWHM. All TiO_2 samples appear in the rutile phase, where the rutile phase is grown in an acidic solvent [13] change in the behavior of rutile in some peaks with changing the concentration of hydrochloric acid, noting a decrease in the crystal size average from 41 nm to 20 nm when increasing the amount of HCl from 1 ml to 1.5 ml [25]. The grain size of specific peaks (110), (101), (111), and (211) of TiO_2 nanostructures

is reduced with an increase in the HCl concentration and a decrease in the etching time. Note that it was not possible to conduct an XRD test on sample H due to the effect of the acid concentration on the amount of the resulting substance, i.e., it is a small amount.

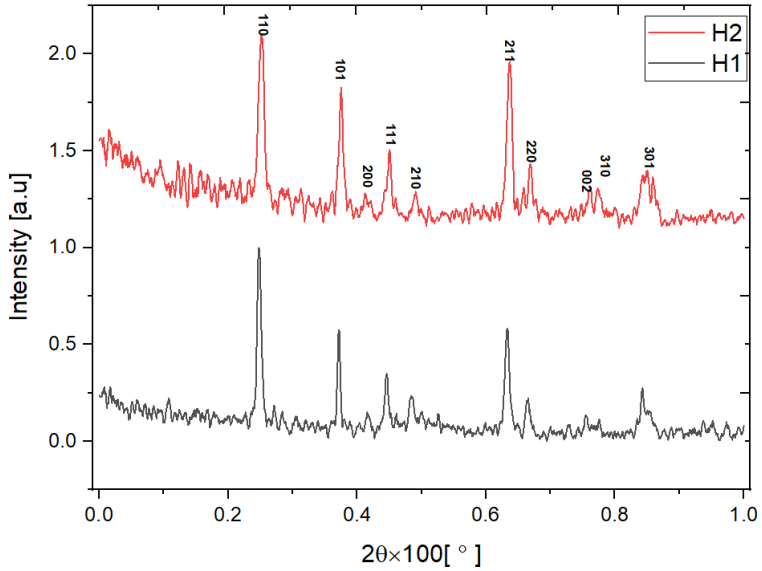

Figure 4. XRD pattern for the TiO_2 prepared sample by using H2=1.5 ml and H1=1 ml.

Table 2. The structural analysis of TiO_2 NPs (HCl=1ml).

2 theta (degree)	Hkl	FWHM (deg)	2 theta (Rad.)	FWHM (Rad)	D(nm)	Matched by
27.37074	110	0.413528	0.239	0.007	19.765	01-077-0441
36.01286	101	0.407096	0.314	0.007	20.512	
39.3925	200	0.135792	0.344	0.002	62.115	
41.23354	111	0.22632	0.360	0.004	37.489	
43.97615	210	0.271584	0.384	0.005	31.534	
54.32209	211	0.45264	0.474	0.008	19.719	
56.44509	220	0.362112	0.493	0.006	24.889	
62.80814	002	0.22632	0.548	0.004	41.110	
68.96941	301	0.22632	0.602	0.004	42.569	
76.2534	202	0.1104	0.665	0.002	91.440	
78.1729	212	0.181056	0.682	0.003	56.507	
				Average	41	

Table 3. The structural analysis of TiO_2 NPs(HCl=1.5ml).

2 theta (degree)	Hkl	FWHM (deg)	2 theta (Rad.)	FWHM (Rad)	D (nm)	Matched by
27.78441	110	0.633696	0.242	0.011	12.909	01-088-1172
36.28295	101	0.271584	0.317	0.005	30.770	
39.17263	200	0.90528	0.342	0.016	9.311	
41.55254	111	0.271584	0.363	0.005	31.274	
44.38239	210	0.45264	0.387	0.008	18.948	
54.617	211	0.724224	0.477	0.013	12.340	
56.83947	220	0.362112	0.496	0.006	24.935	
63.37579	002	0.362112	0.553	0.006	25.772	
64.29815	310	0.602484	0.561	0.011	15.568	
69.25338	301	0.543168	0.604	0.009	17.767	
		Average			20	

The Scherrer formula was used to calculate the crystallite size, which is given in the following equation (11) [29]:

$$\text{Crystallite Size } (D) = K\lambda/\beta \cos\theta \qquad (11)$$

Noting that, D is the crystallite size in nm, K is the shape factor, which is equal to 0.94, λ is the wavelength of X-ray radiation Cu kα1 (λ = 1.5406 Å), and β is the full width half maximum.

3.2. Morphological properties of TiO_2 NPs.

FESEM images showed that the morphological structure and the distribution of TiO_2 nanoparticles on the surface changed simultaneously with changes in the acid concentration in the reaction medium. Where the size of the TiO_2 nanoparticles dropped by increasing the concentration of the HCl, as shown in Figures 5,6. The average particle size of TiO_2 was determined using ImageJ software. The measured particle size of the samples in Table 4.

Table 4. Average particle size of TiO_2 for all samples.

Sample	particle size (nm)
H	41
H1	35
H2	28

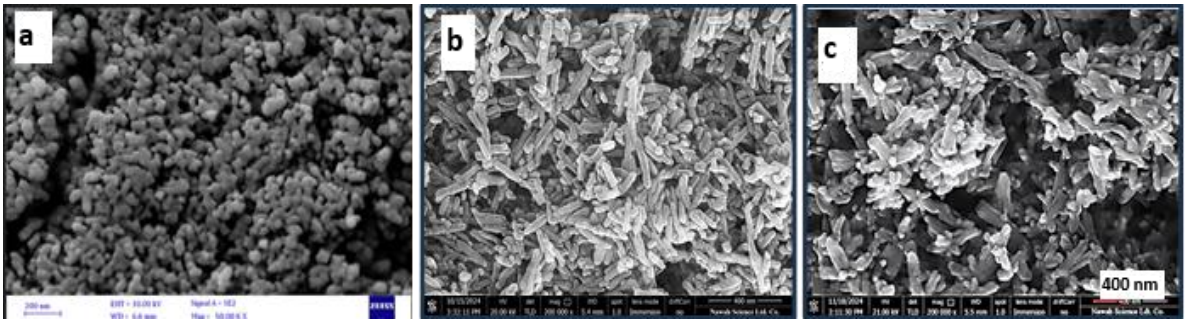

Figure 5. Shows the surface morphology of rutile TiO_2 NPs by field emission scanning electron microscopy at the nm scale: **(a)** H sample; **(b)** H1 sample; **(c)** H2 sample.

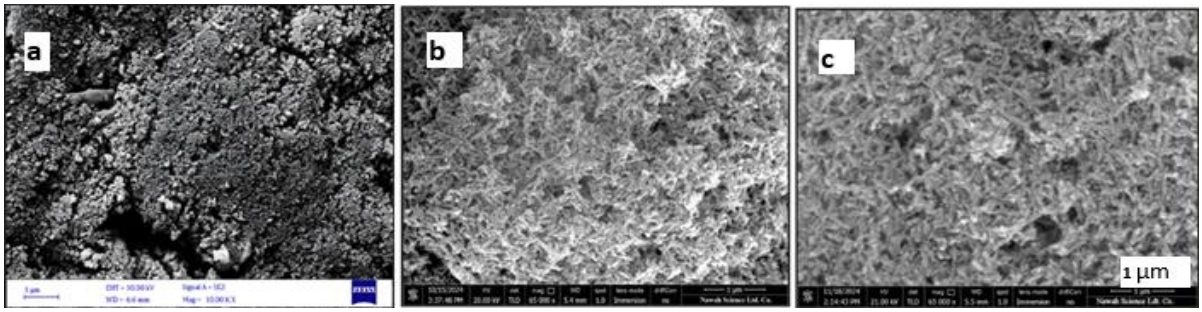

Figure 6. Shows the surface morphology of rutile TiO_2 NPs by field emission scanning electron microscopy at 1µm: **(a)** H sample; **(b)** H1 sample; **(c)** H2 sample.

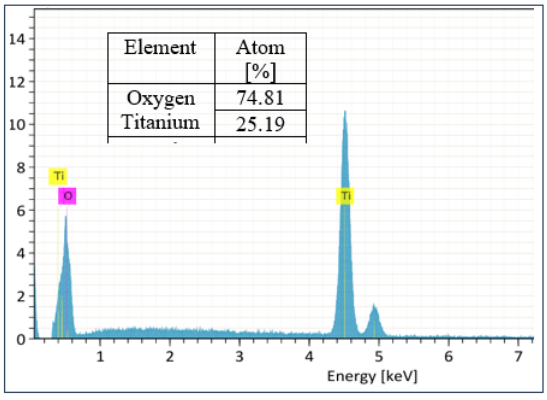

Figure 7. EDX results of TiO_2 nanoparticles.

The chemical composition of titanium dioxide was studied by energy dispersive X-ray (EDX) analysis. Summits confirm in EDX images the formation of high-purity titanium dioxide nanoparticles; the obtained spectrum is shown in Figure 7, which exhibits Ti (25.19%) and O (74.81%) peaks in the prepared rutile TiO_2 NPs nanostructure.

3.3. Electrochemical properties of TiO_2 NPs.

Figure 8 shows the change in zeta potential of titanium dioxide nanoparticles with hydrochloric acid concentration**.** Table 2 shows the results of a Zeta potential technique for measuring the electric charge on the surface (-0.799 to +25 mV) of TiO_2 NPs in a liquid medium. The nanoparticles of TiO_2 repel each other and are less agglomerated due to electrical repulsive forces. Some of these values are very close to the zeta values that indicate the stability of nanoparticles, which are about (±30mV) [40]. From these results, we find that the relationship between zeta potential and acid concentration is non-linear, as shown in Figure 9. Increasing the acid concentration creates a positively charged surface, which is an important factor in the antibacterial effect. As the concentration of HCl increases, we find a decrease in the Zeta deviation (3.92,25.5,4.59 mV), which represents the extent of the deviation from the expected values of the zeta potential, but the increase is irregular, meaning the presence of factors other than the acid concentration, including temperature.

Table 5. Zeta potential results of TiO_2 NPs.

Sample	Zeta potential(mV)	Zeta deviation(mV)
H(HCl=0.75ml)	-0.799	3.92
H1(HCl=1ml)	+25	25.5
H2(HCl=1.5ml)	+24.9	4.59

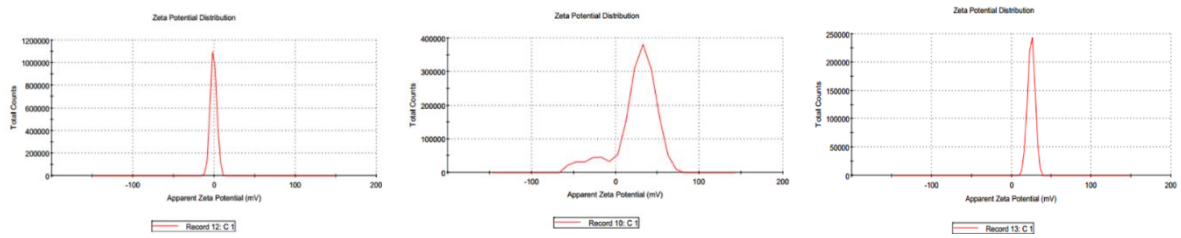

(a) **(b)** **(c)**

Figure 8. Scheme Zeta potential distribution of samples TiO_2 NPs: **(a)** H; **(b)** H1; **(c)** H2.

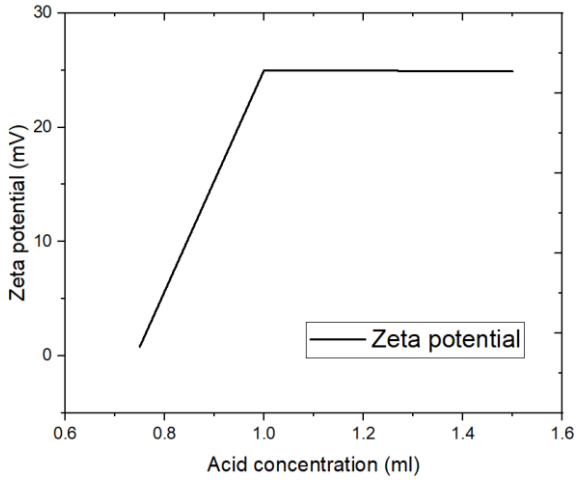

Figure 9. Scheme representing the relationship between the zeta potential and acid concentration of TiO_2 NPs.

3.4. Antibacterial activity.

The antibacterial activity results for 10mg/ml TiO_2 NRs prepared by the solvothermal method with different concentrations (H, H1, H2) are shown in Figure 10, and the details are explained in Table 6, for Gram-negative bacteria (*E. coli*, *K. pneumoniae*) and Gram-positive bacteria (*S.mutans, S. aureus*). The results indicate that the nanoparticles TiO_2 of all samples inhibit the growth of bacteria within 24 hours. The results show a greater effect of sample H2 on inhibiting the growth of all types of bacteria than the other samples (H1, H), and a lesser effect of sample H1. The physical and chemical properties, surface area, shape, and charge of nanoparticles are important parameters that influence their antibacterial properties [33,41]. The antibacterial effect depends on other variables, such as time, concentration, and size, as smaller substances are more toxic than larger ones.

Table 6. The antibacterial activity of TiO_2 NRs.

Sample	E.coli ±0.4mm	S.mutans ±0.2 mm	S.auerus ±0.3mm	K.pneumonia ±0.3mm
H	35	23	23.5	15
H1	16	12	13	10
H2	51	24	26	25

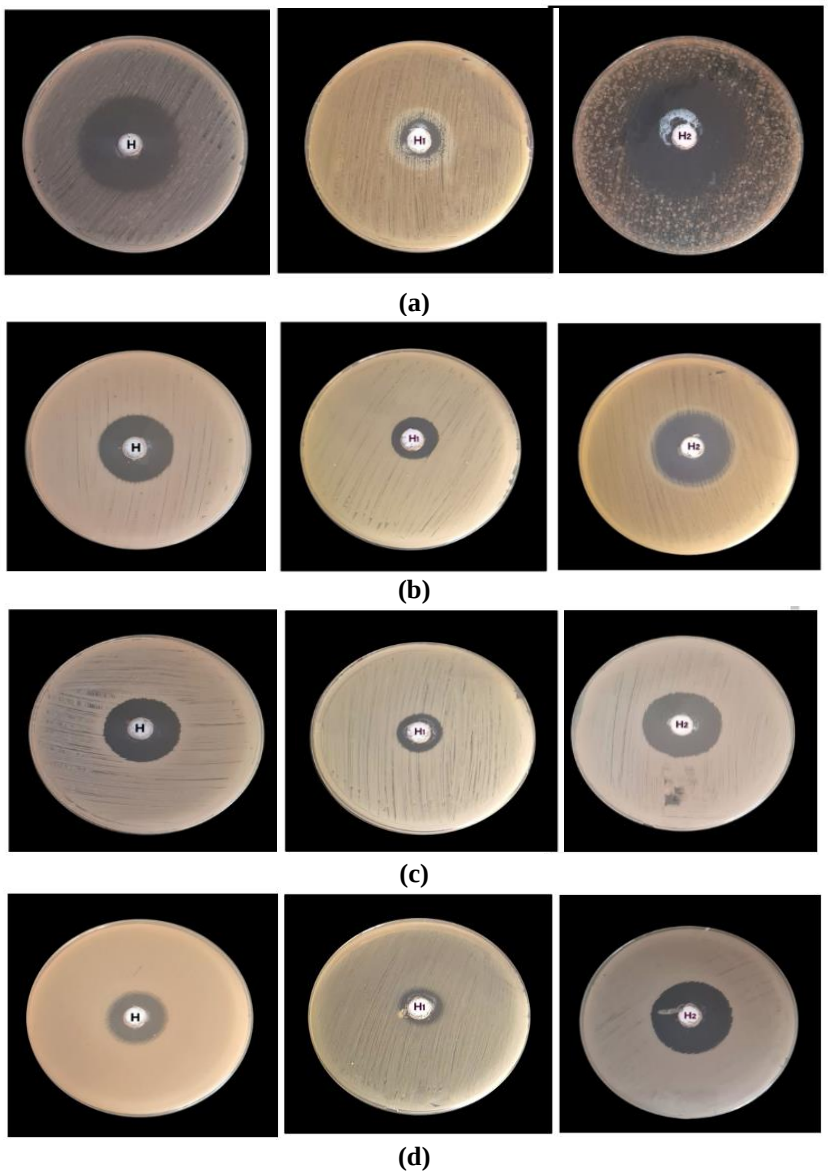

Figure 10. Antibacterial activity of (H2, H1, H) against **(a)** *E. coli*; **(b)** *S. mutans*; **(c)** *S. aureus*; **(d)** *K. pneumonia* at a concentration of 10 mg/mL.

Many factors influence the bacterial cell death mechanism induced by NPs, including size, shape, concentration, electrical charge, surface structure, solvents, and exposure time [42].

4. Conclusion

In conclusion, our procedure uses titanium butoxide as a starting material and varying HCl concentrations to prepare titanium oxide nanorods via the solvothermal method. The variation of HCl concentration leads to a decrease in the preparation temperature. A stable rutile phase structure formed in all samples due to interactions among the substances in an acidic environment. Noting the difference in the appearance time, which caused an increase in the size of the nanorod with a decrease in the acid concentration.

Author Contributions

Author Contributions: Conceptualization, M.A. and A.S.H.; methodology, M.A. and A.S.H.; software, M.A.; validation, M.A. and A.S.H.; formal analysis, M.A. and A.S.H.; investigation, M.A.; resources, M.A.; data curation, M.A.; writing—original draft preparation, M.A.; writing—review and editing, A.S.H. and M.A.; visualization, M.A.; supervision, A.S.H.; project administration, A.S.H.; funding acquisition, M.A. All authors have read and agreed to the published version of the manuscript.

Institutional Review Board Statement

Not applicable.

Informed Consent Statement

Not applicable.

Data Availability Statement

All data generated or analyzed during this study are included in this published article.

Funding

This research received no external funding.

Acknowledgments

A special thanks to the University of Kerbala, College of Science, Department of Physics, for its support and assistance with this work. Also, grateful appreciation is extended to *the Phi Nanoscience Center* for support in analyzing research samples. Their contribution is sincerely acknowledged.

Conflicts of Interest

The author declares no conflict of interest.

Abbreviations

The following abbreviations are used in this manuscript:

Abbreviation	Definition
WS-Ceria-NPs	*Withania somnifera*-derived Cerium Oxide Nanoparticles
ROS	Reactive Oxygen Species
RONS	Reactive Oxygen and Nitrogen Species
SOD	Superoxide Dismutase
DPPH	2,2-diphenyl-1-picrylhydrazyl
LPS	Lipopolysaccharide
SAED	Selected Area Electron Diffraction
FFT	Fast Fourier Transform
HRTEM	High-Resolution Transmission Electron Microscopy
PBS	Phosphate-buffered Saline
BSA	Bovine Serum Albumin
NOX	Nitric Oxide Assay
XRD	X-ray Diffraction
SEM	Scanning Electron Microscopy
EDS/EDX	Energy Dispersive X-ray Spectroscopy
FTIR	Fourier Transform Infrared Spectroscopy
UV-Vis	Ultraviolet-visible Spectroscopy
SD	Standard Deviation
ANOVA	Analysis of Variance

References

1. Khashan, K.S.; Sulaiman, G.M.; Abdulameer, F.A.; Albukhaty, S.; Ibrahem, M.A.; Al-Muhimeed, T.; AlObaid, A.A. Antibacterial activity of TiO_2 nanoparticles prepared by one-step laser ablation in liquid. *Appl. Sci.* **2021**, *11*, 4623, https://doi.org/10.3390/app11104623.
2. Bhullar, S.; Goyal, N.; Gupta, S.J.R.a. Rapid green-synthesis of TiO_2 nanoparticles for therapeutic applications. *RSC Adv.* **2021**, *11*, 30343-30352, https://doi.org/10.1039/d1ra05588g.
3. Adetunji, C.O.; Olaniyan, O.T.; Singh, K.R.B.; Inobeme, A.; Nayak, V.; Singh, J.; Singh, R.P. Role of biopesticides derived from bionanomaterials for enhanced food security and sustainable agriculture. In Bionanomaterials for Environmental and Agricultural Applications; Singh, R.P., Singh, K.R.B., Eds.; IOP Publishing: Bristol, UK, **2021**; 5-1-5-13, https://doi.org/10.1088/978-0-7503-3863-9ch5.
4. Lee, Y.-J.; Jae Jeong, Y.; Sun Cho, I.; Lee, C.-G.; Park, S.-J.; Alvarez, P.J.J. The inhibitory mechanism of humic acids on photocatalytic generation of reactive oxygen species by TiO_2 depends on the crystalline phase. *Chem. Eng. J.* **2023**, *476*, 146785, https://doi.org/10.1016/j.cej.2023.146785.
5. Bano, F.; Bano, F. Green-Synthesized Titanium Dioxide Nanoparticles Inhibit and Eradicate the Biofilms of Pathogenic Bacteria Through Intracellular ROS Production. *Microbiol. Res.* **2025**, *16*, 48, https://doi.org/10.3390/microbiolres16020048.
6. Haji, S.H.; Ganjo, A.R.; Faraj, T.A.; Fatah, M.H.; Smail, S.B.; Haji, S.H.; Ganjo, A.R.; Faraj, T.A.; Fatah, M.H.; Smail, S.B. The enhanced antibacterial and antibiofilm properties of titanium dioxide nanoparticles biosynthesized by multidrug-resistant Pseudomonas aeruginosa. *BMC Microbiol.* **2024**, *24*, 379, https://doi.org/10.1186/s12866-024-03530-y.
7. Laganà, A.; Visalli, G.; Corpina, F.; Ferlazzo, M.; Di Pietro, A.; Facciolà, A. Antibacterial activity of nanoparticles and nanomaterials: a possible weapon in the fight against healthcare-associated infections. *Eur. Rev. Med. Pharmacol. Sci.* **2023**, *27*, 3645-3663, https://doi.org/10.26355/eurrev_202304_32151.
8. Kaushik, S. Editorial: Reviews in antibiotic resistance and new antimicrobial drugs. *Front. Cell. Infect. Microbiol.* **2024**, *14*, 1434140, https://doi.org/10.3389/fcimb.2024.1434140.
9. Alhalili, Z.; Alhalili, Z. Metal Oxides Nanoparticles: General Structural Description, Chemical, Physical, and Biological Synthesis Methods, Role in Pesticides and Heavy Metal Removal through Wastewater Treatment. *Molecules* **2023**, *28*, 3086, https://doi.org/10.3390/molecules28073086.
10. He, L.; Zhang, W.; Liu, J.; Pan, Y.; Li, S.; Xie, Y. Applications of nanotechnology in orthodontics: a comprehensive review of tooth movement, antibacterial properties, friction reduction, and corrosion resistance. *BioMed. Eng. OnLine* **2024**, *23*, 72, https://doi.org/10.1186/s12938-024-01261-9.
11. Martinez, G.; Merinero, M.; Pérez-Aranda, M.; Pérez-Soriano, E.M.; Ortiz, T.; Villamor, E.; Begines, B.; Alcudia, A. Environmental impact of nanoparticles' application as an emerging technology: A review. *Materials* **2020**, *14*, 166, https://doi.org/10.3390/ma14010166.

12. Sheikh, M.; Makkad, S.; Shende, S.; Deshmukh, M. Antimicrobial Efficacy of Metal-Doped Titanium Dioxide Nanoparticles: A Comprehensive Review. *Int. J. Pharm. Investig.* **2024**, *14*, https://doi.org/10.5530/ijpi.14.4.114.
13. Hochvaldová, L.; Večeřová, R.; Kolář, M.; Prucek, R.; Kvítek, L.; Lapčík, L.; Panáček, A. Antibacterial nanomaterials: Upcoming hope to overcome antibiotic resistance crisis. *Nanotechnol. Rev.* **2022**, *11*, 1115-1142, https://doi.org/10.1515/ntrev-2022-0059.
14. Hamrayev, H.; Korpayev, S.; Shameli, K. Advances in Synthesis Techniques and Environmental Applications of TiO_2 Nanoparticles for Wastewater Treatment: A Review. *J. Res. Nanosci. Nanotechnol.* **2024**, *12*, 1–24, https://doi.org/10.37934/jrnn.12.1.124.
15. Younis, A.B.; Milosavljevic, V.; Fialova, T.; Smerkova, K.; Michalkova, H.; Svec, P.; Antal, P.; Kopel, P.; Adam, V.; Zurek, L. Synthesis and characterization of TiO_2 nanoparticles combined with geraniol and their synergistic antibacterial activity. *BMC Microbiol.* **2023**, *23*, 207, https://doi.org/10.1186/s12866-023-02955-1.
16. Armaković, S.J.; Savanović, M.M.; Armaković, S. Titanium dioxide as the most used photocatalyst for water purification: an overview. *Catalysts* **2022**, *13*, 26, https://doi.org/10.3390/catal13010026.
17. Razzaq, Z.; Khalid, A.; Ahmad, P.; Farooq, M.; Khandaker, M.U.; Sulieman, A.; Rehman, I.U.; Shakeel, S.; Khan, A. Photocatalytic and antibacterial potency of titanium dioxide nanoparticles: a cost-effective and environmentally friendly media for treatment of air and wastewater. *Catalysts* **2021**, *11*, 709, https://doi.org/10.3390/catal11060709.
18. Roy, J. The synthesis and applications of TiO_2 nanoparticles derived from phytochemical sources. *J. Ind. Eng. Chem.* **2022**, *106*, https://doi.org/10.1016/j.jiec.2021.10.024.
19. Ulfa, M.; Pangestuti, I.; Anggreani, C.N. Physicochemical Characteristics of Titania Particles Synthesized with Gelatin as a Template Before and After Regeneration and Their Performance in Photocatalytic Methylene Blue. *Bull. Chem. React. Eng. Catal.* **2024**, *19*, https://doi.org/10.9767/bcrec.20138.
20. Serov, D.A.; Gritsaeva, A.V.; Yanbaev, F.M.; Simakin, A.V.; Gudkov, S.V.; Serov, D.A.; Gritsaeva, A.V.; Yanbaev, F.M.; Simakin, A.V.; Gudkov, S.V. Review of Antimicrobial Properties of Titanium Dioxide Nanoparticles. *Int. J. Mol. Sci.* **2024**, *25*, 10519, https://doi.org/10.3390/ijms251910519.
21. Hameed, H.G.; Abdulrahman, N.A. Synthesis of TiO2 Nanoparticles by Hydrothermal Method and Characterization of their Antibacterial Activity: Investigation of the Impact of Magnetism on the Photocatalytic Properties of the Nanoparticles. *Phys. Chem. Res.* **2023**, *11*, https://doi.org/10.22036/pcr.2022.351688.2137.
22. Kim, S.Y.; Saqlain, S.; Cha, B.J.; Zhao, S.; Seo, H.O.; Kim, Y.D. Annealing temperature-dependent effects of Fe-Loading on the visible light-driven photocatalytic activity of rutile TiO_2 nanoparticles and their applicability for air purification. *Catalysts* **2020**, *10*, 739, https://doi.org/10.3390/catal10070739.
23. Sa'aya, N.S.N.; Halim, N.A.; Tajuddin, H.A.; Norrrahim, M.N.F.; Demon, S.Z.N.; Ros, F.C.; Aziz, S.; Hamsan, M.H.; Azmi, A.F.M.; Abidin, N.H.Z. Exploring the effective parameters on the photocatalytic activity of TiO_2 nanoparticles. *S. Afr. J. Chem. Eng.* **2025**, *53*, https://doi.org/10.1016/j.sajce.2025.04.014.
24. Irshad, M.A.; Nawaz, R.; Rehman, M.Z.u.; Adrees, M.; Rizwan, M.; Ali, S.; Ahmad, S.; Tasleem, S. Synthesis, characterization and advanced sustainable applications of titanium dioxide nanoparticles: A review. *Ecotoxicol. Environ. Saf.* **2021**, *212*, https://doi.org/10.1016/j.ecoenv.2021.111978.
25. Wategaonkar, S.B.; Parale, V.G.; Pawar, R.P.; Mali, S.S.; Hong, C.K.; Powar, R.R.; Moholkar, A.V.; Park, H.H.; Sargar, B.M.; Mane, R.K. Structural, morphological, and optical studies of hydrothermally synthesized Nb-added TiO_2 for DSSC application. *Ceram. Int.* **2021**, *47*, 25580-25592, https://doi.org/10.1016/j.ceramint.2021.05.284.
26. Domingues, L.A.; Carriello, G.M.; Pegoraro, G.M.; Mambrini, G.P. Synthesis of TiO_2 nanoparticles by the solvothermal method and application in the catalysis of esterification reactions. *An. Acad. Bras. Cienc.* **2024**, *96*, e20240096, https://doi.org/10.1590/0001-3765202420240096.
27. Hsu, C.-Y.; Mahmoud, Z.H.; Abdullaev, S.; Ali, F.K.; Naeem, Y.A.; Mizher, R.M.; Karim, M.M.; Abdulwahid, A.S.; Ahmadi, Z.; Habibzadeh, S. Nano titanium oxide (nano-TiO_2): A review of synthesis methods, properties, and applications. *Case Stud. Chem. Environ. Eng.* **2024**, *9*, 100626, https://doi.org/10.1016/j.cscee.2024.100626.
28. Xu, X.; Xiao, Y.; Zhao, R.; Yin, Z.; Butt, H.A.; Li, M.; Wang, Z. Tailored TiO2/WO3 composites for enhanced electrocatalytic and photocatalytic applications. *Ceram. Int.* **2025**, *51*, https://doi.org/10.1016/j.ceramint.2025.01.203.

29. Ismail, W.; Ibrahim, G.; Atta, H.; Sun, B.; El-Shaer, A.; Abdelfatah, M. Improvement physical and photoelectrochemical properties of TiO2 nanorods toward biosensor and optoelectronic applications. *Ceram. Int.* **2024**, *50*, https://doi.org/10.1016/j.ceramint.2024.02.286.
30. Yang, H.; Yang, B.; Chen, W.; Yang, J.; Yang, H.; Yang, B.; Chen, W.; Yang, J. Preparation and Photocatalytic Activities of TiO2-Based Composite Catalysts. *Catalysts* **2022**, *12*, 1263, https://doi.org/10.3390/catal12101263.
31. Jabar, B.A.; Yaseen, H.M.; Hamzah, M.A.; Tahir, K.J.; Ridha, N.J.; Alosfur, F.K.M.; Madlol, R.A.; Hussein, B.M. Synthesis and Structural Properties of Eu^{3+}:TiO_2 Nanoparticles. *J. Nanostructures* **2021**, *11*, 136-142, https://doi.org/10.22052/JNS.2021.01.015.
32. Prathan, A.; Sanglao, J.; Wang, T.; Bhoomanee, C.; Ruankham, P.; Gardchareon, A.; Wongratanaphisan, D. Controlled Structure and Growth Mechanism behind Hydrothermal Growth of TiO_2 Nanorods. *Sci. Rep.* **2020**, *10*, 8065, https://doi.org/10.1038/s41598-020-64510-6.
33. Querebillo, C.J.; Querebillo, C.J. A Review on Nano Ti-Based Oxides for Dark and Photocatalysis: From Photoinduced Processes to Bioimplant Applications. *Nanomaterials* **2023**, *13*, 982, https://doi.org/10.3390/nano13060982.
34. Ozdal, M.; Gurkok, S. Recent advances in nanoparticles as antibacterial agent. *ADMET DMPK* **2022**, *10*, 115–129, https://doi.org/10.5599/admet.1172.
35. Chandoliya, R.; Sharma, S.; Sharma, V.; Joshi, R.; Sivanesan, I.; Chandoliya, R.; Sharma, S.; Sharma, V.; Joshi, R.; Sivanesan, I. Titanium Dioxide Nanoparticle: A Comprehensive Review on Synthesis, Applications and Toxicity. *Plants* **2024**, *13*, 2964, https://doi.org/10.3390/plants13212964.
36. Gupta, T.; Cho, J.; Prakash, J. Hydrothermal synthesis of TiO_2 nanorods: formation chemistry, growth mechanism, and tailoring of surface properties for photocatalytic activities. *Mater. Today Chem.* **2021**, *20*, https://doi.org/10.1016/j.mtchem.2021.100428.
37. Javed, R.; Ain, N.u.; Gul, A.; Ahmad, M.A.; Guo, W.; Ao, Q.; Tian, S. Diverse biotechnological applications of multifunctional titanium dioxide nanoparticles: An up-to-date review. *IET Nanobiotechnol.* **2022**, *16*, 171-189, https://doi.org/10.1049/nbt2.12085.
38. Garzon-Roman, A.; Sanchez-Mora, E.; Romero-López, A.; de Anda-Reyes, M.E.; Zúñiga-Islas, C.; Garzon-Roman, A.; Sanchez-Mora, E.; Romero-López, A.; de Anda-Reyes, M.E.; Zúñiga-Islas, C. Porous Silicon Working as Immobilizer of TiO2 Decorated with Metal Nanoparticles Analyzing the Absorber and Photocatalytic Activity for Dexamethasone. *Silicon* **2025**, *17*, 1253-1266, https://doi.org/10.1007/s12633-025-03264-0.
39. Bilek, O.; Fialova, T.; Otahal, A.; Adam, V.; Smerkova, K.; Fohlerova, Z. Antibacterial activity of AgNPs–TiO2 nanotubes: influence of different nanoparticle stabilizers. *RSC Adv.* **2020**, *10*, 44601-44601, https://doi.org/10.1039/D0RA07305A.
40. Ali, A.; Chiang, Y.W.; Santos, R.M.; Ali, A.; Chiang, Y.W.; Santos, R.M. X-ray Diffraction Techniques for Mineral Characterization: A Review for Engineers of the Fundamentals, Applications, and Research Directions. *Minerals* **2022**, *12*, 205, https://doi.org/10.3390/min12020205.
41. Chen, D.; Martínez, V.A.; Vasco, D.A.; Guzmán, A.M. Experimental investigation of viscosity, enhanced thermal conductivity and zeta potential of a TiO2 electrolyte – based nanofluid. *Int. Commun. Heat Mass Transf.* **2020**, *118*, https://doi.org/10.1016/j.icheatmasstransfer.2020.104840.
42. Baptista, P.V.; McCusker, M.P.; Carvalho, A.; Ferreira, D.A.; Mohan, N.M.; Martins, M.; Fernandes, A.R. Nano-Strategies to Fight Multidrug Resistant Bacteria—"A Battle of the Titans". *Front. Microbiol.* **2018**, *9*, 1441, https://doi.org/10.3389/fmicb.2018.01441.
43. Guo, Z.; Liu, H.; Wang, W.; Hu, Z.; Li, X.; Chen, H.; Wang, K.; Li, Z.; Yuan, C.; Ge, X. Recent advances in antibacterial strategies based on TiO2 biomimetic micro/nano-structured surfaces fabricated using the hydrothermal method. *Biomimetics* **2024**, *9*, 656, https://doi.org/10.3390/biomimetics9110656.

Publisher's Note & Disclaimer

instructions, or products mentioned in the content. Readers are encouraged to independently verify any information before relying on it, and the publisher assumes no responsibility for any consequences arising from the use of materials contained in this publication.